Validity of the Born-Oppenheimer approximation in the indirect-dissociative-recombination process

Roman Čurík*
J. Heyrovský Institute of Physical Chemistry, ASCR, Dolejškova 3, 18223 Prague, Czech Republic

Dávid Hvizdoš
J. Heyrovský Institute of Physical Chemistry, ASCR, Dolejškova 3, 18223 Prague, Czech Republic and Institute of Theoretical Physics, Faculty of Mathematics and Physics, Charles University in Prague, V Holešvičkách 2, 180 00 Prague, Czech Republic

Chris H. Greene
Department of Physics and Astronomy, Purdue University, West Lafayette, Indiana 47907, USA

(Received 23 October 2018; published 11 December 2018)

An alternative method is introduced to solve a simple two-dimensional model describing vibrational excitation and dissociation processes during the electron-molecule collisions. The model works with one electronic and one nuclear degree of freedom. The two-dimensional R matrix can be constructed simultaneously on the electronic and nuclear surfaces using all three forms developed previously for electron-atom and electron-molecule collisions. These are the eigenchannel R-matrix form, inversion technique of Nesbet and Robicheaux, and the Wigner-Eisenbud-type form using expansion over the poles of the symmetrized Hamiltonian. The 2D R-matrix method is employed to solve a simple model tailored to describe the dissociative recombination and the vibrational excitation of H_2^+ cation in the singlet ungerade symmetry $^1\Sigma_u$. These results then serve as a (near-exact) benchmark for the following calculation in which the R-matrix states are replaced by their Born-Oppenheimer approximations. The accuracy of this approach and its correction with the first-order nonadiabatic couplings are discussed.

DOI: 10.1103/PhysRevA.98.062706

I. INTRODUCTION

Presently there are two generally accepted mechanisms for the dissociative recombination (DR) of molecular cations. The *direct* mechanism involves crossing of the potential curves of the target system and of the formed neutral molecule [1]. For several decades this resonant mechanism influenced the theoretical research and molecular systems without the curve crossing were assumed to have small DR rates that were often just estimated [2] in early universe chemistry models.

With the increasing number of experimental data in the early 1990s, it became difficult to support this picture in which the curve crossing is required to drive the DR process. The first theoretical models by Guberman [3] and by Sarpal *et al.* [4] made it clear that the *indirect* mechanism, while not requiring a curve crossing, can be quite effective. Further theoretical studies revealed that even for systems with a curve crossing the DR rate can be enhanced [5,6] or suppressed [7,8] by orders of magnitude when Rydberg states trigger the initial capture (indirect mechanism).

The vast majority of calculations treating the indirect mechanism (as examples see Refs. [9–14] and the references therein) employ the quantum defect theory (QDT) in combination with the (ro)vibrational frame transformation (FT) theory [15]. The frame transformation approach exploits the Born-Oppenheimer approximation (BOA) that is assumed to be valid at small electronic distances. The credibility of the FT theory was often tested by experiments dealing with the elastic and rovibrationally inelastic collisions of electrons with molecules. However, it is more difficult to carry out similar comparison for the dissociative recombination process, because detection of the neutral fragments is more complicated. Moreover, the target molecular cations are often warmed after they are ionized, and possess an unknown rovibrational temperature (or distribution) before the recombination process takes place [16]. General agreement between DR theory and experiment has frequently been limited to an order of magnitude and only rarely have detailed experimental features been reproduced [17,18]. Recent experimental improvements [19], however, have the potential to put the DR theory based on the BOA to a quantitative test.

In order to assess the accuracy of the Born-Oppenheimer approximation, the cornerstone of the vibrational frame-transformation theories [15,20–22], we propose a numerically solvable two-dimensional (2D) model for the indirect-dissociative recombination of H_2 in the singlet ungerade channels $^1\Sigma_u$. This model was recently devised by Hvizdoš *et al.* [23] to test the accuracy of the energy-independent frame transformation into a nuclear basis of Siegert pseudostates. That study thus provided a first numerical estimate for the accuracy of the underlying approximations. The numerically solvable model was based on the exterior complex scaling (ECS) applied to both nuclear and electronic coordinates.

*roman.curik@jh-inst.cas.cz

The ECS approach was originally developed to address the dissociative electron attachment and the vibrational excitation channels in collisions of electrons with neutral molecules [24,25]. For the target cations the ECS method still provided accurate and converged results for most of the collision energies [23], but at comparatively high computational cost due to the necessity of using extensive long-range electronic grids to confine the countless number of Rydberg states involved in the closed-channel resonances.

To overcome these difficulties we propose a 2D R-matrix method that numerically solves the electronic-nuclear problem in a 2D box. The size of this box is determined by the range of the interaction that couples the two degrees of freedom. Outer regions, in which either the electron moves in a pure Coulomb field (or zero field in case of the neutral targets) or the nuclei move in a constant potential, are treated analytically. This is done by application of the multichannel quantum defect theory (MQDT) [26,27] which is slightly extended to eliminate closed channels on both the electronic and nuclear surfaces simultaneously.

Finally, the Born-Oppenheimer approximation of the 2D R matrix is also tested in order to assess the validity of the BOA for the indirect DR process. The BOA version of the R matrix was originally proposed by Schneider *et al.* [28] for electron collisions with diatomic molecules. It was applied to explain the boomerang structures in elastic and vibrationally inelastic electron-N_2 [29,30], and electron-CO [31] collisions. Later the method was revived to treat the vibrational excitation of molecular cations [32,33] and even the DR channel of HeH^+ [4].

II. 2D R MATRIX

A. The 2D model

The 2D Hamiltonian partitioning is adopted from Ref. [23] and it is somewhat different from the original notation of Houfek *et al.* [24,25]. The present system, with two different modes of fragmentation, associated with the competing dissociation and ionization (or detachment) channels, will be described by the time-independent Schrödinger equation,

$$[H_{\rm n}(R) + H_{\rm e}(r) + V(R,r) - E]\psi(R,r) = 0, \qquad (1)$$

where

$$H_{\rm n}(R) = -\frac{1}{2M}\frac{\partial^2}{\partial R^2} + V_0(R), \qquad (2)$$

$$H_{\rm e}(r) = -\frac{1}{2}\frac{\partial^2}{\partial r^2} + \frac{l(l+1)}{2r^2} - \frac{Z}{r}. \qquad (3)$$

The potential curve $V_0(R)$ describes the vibrational motion of the target molecule. The interaction potential $V(R,r)$ couples the electronic and nuclear degrees of freedom with the following asymptotic limits:

$$V(R,r) = 0 \quad \text{for} \quad r \geqslant r_0, \qquad (4)$$

$$V(R,r) = V(R_0,r) \quad \text{for} \quad R \geqslant R_0. \qquad (5)$$

In the present study, V_0 is chosen to be the Morse potential describing the ground state of $H_2{}^+$, and $V(R,r)$ is tailored to reproduce approximately the $^1\Sigma_u$ quantum defects of the neutral hydrogen molecule H_2. The explicit form of the two potentials can be found in Ref. [23]. The charge parameter is $Z = 0$ for neutral target molecules, while $Z = 1$ for target cation. The angular degrees of freedom have already been separated in spherical coordinates, such that the full solution in the inner region (reaction zone in Fig. 1) is given by

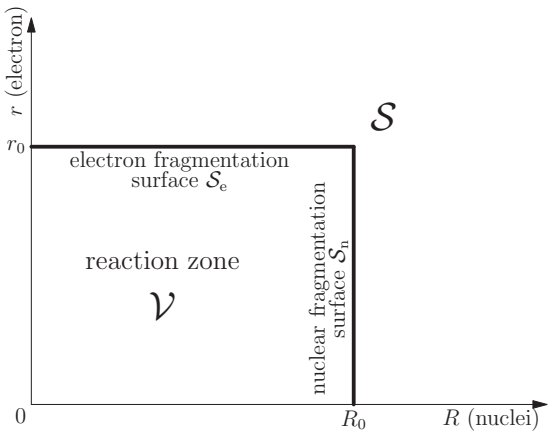

FIG. 1. Partitioning of the configuration space into inner and outer regions.

$$\Psi(\boldsymbol{R},\boldsymbol{r}) = \frac{1}{Rr}\psi(R,r)\Phi(\boldsymbol{\Omega}), \qquad (6)$$

where the symbol $\boldsymbol{\Omega}$ represents all the angular degrees of freedom. In fact, the possibility of additional partial waves and electronic symmetries would require a sum over multiple channels Φ resulting in a coupled set of equations (1). In the present study the 2D R-matrix method will be applied to a model describing the dissociative recombination of $H_2{}^+$ in the singlet ungerade symmetry. It is sufficient to assume [34] that only the p-wave channel is active for the electronic coordinate. The nuclear coordinate R is confined to s-wave scattering and bound vibrational states.

Before we proceed, it is convenient [35] to absorb the mass factor M in Eq. (2) by rescaling of the nuclear coordinate to $X = \sqrt{M}R$. The change of the nuclear variable recasts the full 2D Hamiltonian into a more symmetric form giving

$$\left[H_{\rm n}(X) + H_{\rm e}(r) + V\left(\frac{X}{\sqrt{M}}, r\right) - E\right]\psi(X,r) = 0, \qquad (7)$$

with

$$H_{\rm n}(X) = -\frac{1}{2}\frac{\partial^2}{\partial X^2} + V_0\left(\frac{X}{\sqrt{M}}\right). \qquad (8)$$

For the sake of brevity the potentials in the above equations will be denoted simply as $V(X,r)$ and $V_0(X)$.

B. Eigenchannel R matrix

Formally, the Schrödinger equation (7) describes two interacting distinguishable particles having the same mass of the electron. In such a case the eigenvalues $b(E)$ of the two-particle logderivative operator $\mathcal{B}(E)$ satisfy the following variational principle [36]:

$$b(E) = 2\,\underset{\psi}{\rm stat}\left\{\frac{\langle\psi|\bar{H} - E|\psi\rangle}{\langle\psi|\psi\rangle}\right\}, \qquad (9)$$

where the symmetrized Hamiltonian $\bar{H}$ is defined as

$$\bar{H} = H + \frac{1}{2}\left[\delta(X - X_0)\frac{\partial}{\partial X} + \delta(r - r_0)\frac{\partial}{\partial r}\right], \quad (10)$$

$$H = H_{\rm n}(X) + H_{\rm e}(r) + V(X, r), \quad (11)$$

with $X_0 = \sqrt{M}R_0$. The scalar product $\langle\psi|\psi\rangle$ is carried out in the two-particle volume $\mathcal{V} = \langle 0, X_0\rangle \times \langle 0, r_0\rangle$ [36] and the scalar product denoted by $(\psi|\psi)$ is carried out on the two-particle surface $\mathcal{S}$ enclosing the volume $\mathcal{V}$. If a surface delta function $\delta(\mathcal{S})$ is defined as

$$\delta(\mathcal{S}) = \delta(X - X_0) + \delta(r - r_0), \quad (12)$$

we can simply write

$$(\psi|\psi) = \langle\psi|\delta(\mathcal{S})|\psi\rangle. \quad (13)$$

The stationary principle (9) leads to the Schrödinger equation for the eigenvalues $b_\alpha(E)$,

$$2(\bar{H} - E)|\psi_\alpha\rangle = b_\alpha\,|\psi_\alpha) = b_\alpha\,\delta(\mathcal{S})|\psi_\alpha\rangle. \quad (14)$$

The logderivative operator $\mathcal{B}(E)$ and the inverse operator $\mathcal{R}(E) = \mathcal{B}^{-1}(E)$ operate on a class of functions defined on the surface $\mathcal{S}$. In the case these functions are formed by surface values of $\psi(X, r)$ satisfying the 2D Schrödinger equation (7), these operators become Hermitian [36]. The eigenfunctions $\psi_\alpha(X, r)$ are those solutions of (7) that in addition have common outward normal logarithmic derivative b_α on the whole surface $\mathcal{S}$. They allow a formal spectral decomposition of $\mathcal{B}(E)$ and $\mathcal{R}(E)$ as

$$\mathcal{B} = \sum_\alpha |\psi_\alpha)\, b_\alpha\, (\psi_\alpha|, \quad (15)$$

$$\mathcal{R} = \sum_\alpha |\psi_\alpha)\, b_\alpha^{-1}\, (\psi_\alpha|. \quad (16)$$

The form of Eq. (16) requires a special note related to the eigensolutions $\psi_\alpha(X, r)$ of Eq. (14). Since the surface operator $\delta(\mathcal{S})$ on the right-hand side of Eq. (14) has a lower rank than the symmetrized Hamiltonian on the left-hand side there will be, in general, many trivial solutions [27] with the eigenvalues $b_\alpha = 0$. While these trivial solutions do not contribute to the spectral form of $\mathcal{B}$ in Eq. (15) they need to be excluded in the form (16).

The R matrix consists of matrix elements of the $\mathcal{R}$ operator in the basis of functions orthonormal on the surface $\mathcal{S}$. This basis, also called the fragmentation channel functions, can be assembled from two sets of the surface solutions. The first set $\phi_{i_{\rm e}}(X)$ is defined on the electronic surface $\mathcal{S}_{\rm e}$ (see Fig. 1),

$$H_{\rm n}(X)\phi_{i_{\rm e}}(X) = E_{i_{\rm e}}\phi_{i_{\rm e}}(X), \quad (17)$$

while the second set of surface solutions $\rho_{i_{\rm n}}(r)$ is defined on the nuclear surface $\mathcal{S}_{\rm n}$,

$$[H_{\rm e}(r) + V(X_0, r)]\rho_{i_{\rm n}}(r) = E_{i_{\rm n}}\rho_{i_{\rm n}}(r). \quad (18)$$

The channels $|i)$ can be then defined on the whole surface $\mathcal{S}$ by a union of the two sets ($i = \{i_{\rm e}, i_{\rm n}\}$):

$$i \in i_{\rm e}:\ |i) = |\phi_{i_{\rm e}}) \text{ on } \mathcal{S}_{\rm e} \text{ and } |i) = 0 \text{ on } \mathcal{S}_{\rm n}, \quad (19)$$

$$i \in i_{\rm n}:\ |i) = |\rho_{i_{\rm n}}) \text{ on } \mathcal{S}_{\rm n} \text{ and } |i) = 0 \text{ on } \mathcal{S}_{\rm e}. \quad (20)$$

Continuity of the channel states $|i)$ on the surface $\mathcal{S}$ sets the boundary conditions for the channel functions: $\phi_{i_{\rm e}}(X_0) = 0$ and $\rho_{i_{\rm n}}(r_0) = 0$. Finally, the R-matrix elements in these physically motivated channels take the simple form in the eigenchannel expression,

$$R_{ij} = (i|\mathcal{R}|j) = \sum_\alpha (i|\psi_\alpha)\, b_\alpha^{-1}\, (\psi_\alpha|j). \quad (21)$$

C. Resolvent form

The eigenchannel form (21) of the R matrix is expressed in terms of the eigenvalues and eigenvectors of the logderivative surface operator $\mathcal{B}$. The resolvent form was given for the one-particle surface by Nesbet [37] and by Robicheaux [38]. Its generalization for the present two-particle surface is straightforward. It is mathematically less awkward here to introduce a 2D basis set $y_k(R, r)$ in the volume $\mathcal{V}$. The basis set allows us to express the R matrix (21) by an inversion defined in the volume,

$$R_{ij} = \frac{1}{2}\sum_{k,l}(i|y_k)(\Gamma^{-1})_{kl}(y_l|j), \quad (22)$$

where

$$\Gamma_{kl}(E) = \langle y_k|(\bar{H} - E)|y_l\rangle. \quad (23)$$

Both expressions (22) and (21) are variational forms of the R matrix. However, the resolvent form (22) is somewhat easier to implement because it requires only a straightforward inversion (or in practice an inhomoheneous linear system solution) of the $(\bar{H} - E)$ term expressed in the 2D basis. Evaluation through the eigenchannel expression (21), on the other hand, requires a solution of the generalized eigenvalue problem with a singular matrix on the right-hand side of Eq. (14) complemented by a removal of the trivial solutions. This removal procedure may become problematic if the eigenvalue b_α of a nontrivial solution ψ_α approaches zero value.

Both R-matrix forms (22) and (21) become computationally demanding in situations in which the R matrix needs to be evaluated repeatedly for many total energies E. In such cases, the Wigner-Eisenbud expansion over the poles of $\bar{H}$ is more efficient.

D. Wigner-Eisenbud expansion

Equivalence of the Wigner-Eisenbud [39] expansion of the R matrix and its resolvent form (22) was demonstrated, for the one-particle surface, by Robicheaux [38]. The present two-particle case follows closely the same idea of a spectral decomposition of the operator,

$$(\bar{H} - E)^{-1} = \sum_p \frac{|\psi_p\rangle\langle\psi_p|}{E_p - E}, \quad (24)$$

where the eigenstates $|\psi_p\rangle$ and eigenvalues E_p are defined by

$$\bar{H}|\psi_p\rangle = E_p|\psi_p\rangle. \quad (25)$$

Combination of Eqs. (22) and (24) leads to the Wigner-Eisenbud expansion of the R matrix, which can be written in

a form independent of the basis set, as

$$R_{ij} = \frac{1}{2}\sum_p \frac{(i|\psi_p)\,(\psi_p|j)}{E_p - E}. \tag{26}$$

It is important to emphasize that the eigenstates $|\psi_\alpha\rangle$ of Eqs. (14)–(16) and $|\psi_p\rangle$ of Eqs. (24)–(26) are different. While $|\psi_\alpha\rangle$ solve the Schrödinger equation (7) for a given total energy E, the states $|\psi_p\rangle$ satisfy this equation only for $E = E_p$. Even for these discrete energies the two sets of eigenstates differ as they possess different boundary conditions on the surface $\mathcal{S}$.

E. Adiabatic expansion

All three of the R-matrix forms presented in Secs. II B, II C, and II D provide information on the surface logarithmic derivative of the exact 2D model solution. In order to assess validity of the Born-Oppenheimer approximation, we expand the exact 2D eigenstates $\psi_p(X, r)$ in Eqs. (25) and (26) into the fixed-nuclei solutions $\psi_k(r; X)$ as follows:

$$\psi_p(X, r) = \sum_{k'} \psi_{k'}(r; X)\phi_{k'p}(X), \tag{27}$$

where the electronic solutions diagonalize the fixed-nuclei Hamiltonian,

$$[\bar{H}_e(r) + V(X, r)]\psi_k(r; X) = \bar{E}_k(X)\psi_k(r; X), \tag{28}$$

and the nuclear functions $\phi_{k'p}(X)$ result from the coupled set of nuclear Schrödinger equations,

$$[\bar{H}_n + \bar{E}_k(X) - E_p]\phi_{kp}(X) = -\frac{1}{2}\sum_{k'}\left[V^{(1)}_{kk'}(X) + V^{(2)}_{kk'}(X)\right]\phi_{k'p}(X). \tag{29}$$

The first-order nonadiabatic coupling operator for the symmetrized Hamiltonian $\bar{H}$ can be written as

$$V^{(1)}_{kk'}(X) = \left|\frac{d}{dX}\right\rangle\langle\psi_k|\psi'_{k'}\rangle_r + \langle\psi'_k|\psi_{k'}\rangle_r\left\langle\frac{d}{dX}\right|, \tag{30}$$

where $\psi'_k = \partial\psi_k(r; X)/\partial X$ and the scalar product $\langle.|.\rangle_r$ is carried out only on the electronic coordinate r. The first-order nuclear derivative in the first term acts "to the left," e.g., when matrix elements in the nuclear basis are evaluated. The second-order nonadiabatic terms have the form of local potentials,

$$V^{(2)}_{kk'}(X) = \langle\psi'_k|\psi'_{k'}\rangle_r. \tag{31}$$

Finally, the symmetrized nuclear and electronic Hamiltonians $\bar{H}_n$ and $\bar{H}_e$ are obtained by splitting the Bloch operator on the right-hand side of Eq. (10) into respective nuclear and electronic parts, i.e.,

$$\bar{H}_n(X) = H_n(X) + \frac{1}{2}\delta(X - X_0)\frac{\partial}{\partial X}, \tag{32}$$

$$\bar{H}_e(r) = H_e(r) + \frac{1}{2}\delta(r - r_0)\frac{\partial}{\partial r}. \tag{33}$$

The Born-Oppenheimer approximation neglects the nonadiabatic couplings $V^{(1)}_{kk'}$ and $V^{(2)}_{kk'}$. In this case the set of equations (29) decouple and only one term survives in expansion (27),

$$\psi^{BO}_p(X, r) = \psi_k(r; X)\phi_{kn}(X), \tag{34}$$

where $p \equiv \{k, n\}$ represents a combined index of electronic states (indexed by k) and nuclear states (indexed by n). The R matrix,

$$R^{BO}_{ij} = \frac{1}{2}\sum_p \frac{\left(i|\psi^{BO}_p\right)\left(\psi^{BO}_p|j\right)}{E_p - E}, \tag{35}$$

based on the Born-Oppenheimer states was introduced previously for the diatomic molecules by Schneider *et al.* [28].

In the final note of this section we would like to discuss the radius r_0 of the electronic box beyond which we assume $V(X, r) = 0$. On one side we would prefer to have r_0 as small as possible to improve accuracy of the Born-Oppenheimer R matrix (35). On another side, for very small r_0 values, the electronic channels $\rho_{i_n}(r)$ may not fit into the nuclear fragmentation surface $\mathcal{S}_n$ (see Fig. 1). This issue was previously discussed by Jungen [40] where the author introduced radius r_2 as a "distance where all relevant bound Rydberg components have fallen exponentially to a negligibly small value." In the present study the first two electronic states are open already at zero collision energy and they barely fit into the box size of $r_2 = 20$ bohr, while $V(X, r)$ can be considered zero beyond $r_0 = 6$–7 bohr. Therefore, these two contradicting requirements lead to a question, namely whether an R matrix determined in a small 2D box confined by r_0 can be losslessly propagated onto a surface of a larger 2D box confined by r_2, while the nuclear box size X_0 does not change. Such a technique for one-dimensional R-matrix propagation was developed by Baluja *et al.* [41]. The generalization of this procedure for propagation of the 2D R matrix, needed for the present problem, can be found in the appendix.

F. Outer region (cation case)

In this study we do not attempt to solve a dissociative scattering problem in which $R \to \infty$ and $r \to \infty$ simultaneously. Instead, we assume that at least one of the coordinates R or r is confined to the range $R \leqslant R_0$ or $r \leqslant r_0$, respectively. This restriction is also reflected in the choice of the surface channels (19) and (20) that always vanish at the point where $\mathcal{S}_n$ and $\mathcal{S}_e$ meets. In the following we consider N_e channel functions $\phi_{i_e}(X)$ on the electronic surface $\mathcal{S}_e$ and N_n channel functions $\rho_{i_n}(r)$ on the nuclear surface $\mathcal{S}_n$. Therefore, the total number of the surface channels defined by Eqs. (19) and (20) is $N_e + N_n$.

Because the Hamiltonian (11) becomes separable on the surface $\mathcal{S}$, the solutions in the outer regions are made as a sum of products of the channel functions and of the asymptotic solutions. The two independent electronic solutions describing the electronic fragmentation in the Coulomb field will be denoted as $f(r)$ and $g(r)$. Analytic properties of the Coulomb functions (f, g) are detailed completely by Seaton [26] [who calls them $(s, -c)$ functions]. For positive channel energies $\epsilon_{i_e} = E - E_{i_e}$ they have an asymptotic limit of harmonic

functions with the energy normalization,

$$f_{i_e}(r) \to \left(2/\pi k_{i_e}\right)^{1/2} \sin\left(k_{i_e} r + \left(1/k_{i_e}\right) \ln r + \eta\right), \quad (36)$$

$$g_{i_e}(r) \to -\left(2/\pi k_{i_e}\right)^{1/2} \cos\left(k_{i_e} r + \left(1/k_{i_e}\right) \ln r + \eta\right), \quad (37)$$

where $\eta(k_{i_e}, l)$ is a long-range phase shift [27] and the channel momenta are defined by $k_{i_e}^2/2 = \epsilon_{i_e}$. For negative channel energies both functions $f_{i_e}(r)$ and $g_{i_e}(r)$ contain exponentially growing and decaying parts [26,27].

For the asymptotic region beyond the nuclear fragmentation surface $\mathcal{S}_n$ we use zero-field s-wave radial functions,

$$F^0_{i_n}(X) \to (2/\pi)^{1/2} K_{i_n}^{-1} \sin\left(K_{i_n} X\right), \quad (38)$$

$$G^0_{i_n}(X) \to -(2/\pi)^{1/2} \cos\left(K_{i_n} X\right), \quad (39)$$

for positive $\epsilon_{i_n} = E - E_{i_n}$ and

$$F^0_{i_n}(X) \to (1/2\pi)^{1/2} \kappa_{i_n}^{-1} \left(e^{\kappa_{i_n} X} - e^{-\kappa_{i_n} X}\right), \quad (40)$$

$$G^0_{i_n}(X) \to -(1/2\pi)^{1/2} \left(e^{\kappa_{i_n} X} + e^{-\kappa_{i_n} X}\right), \quad (41)$$

for the negative $\epsilon_{i_n} = -\kappa_{i_n}^2/2$. The asymptotic functions F^0_i and G^0_i are not energy normalized, however, they can be smoothly continued through the zero channel energy. Eventually, the wave function for fragmentation regions will be written in terms of the energy-normalized nuclear asymptotic functions, but the respective transformation will be postponed to the later stage of the present treatment of the outer region. If the diagonal matrices for the asymptotic functions evaluated on the whole surface $\mathcal{S}$ are constructed as follows,

$$\underline{\mathcal{F}} = \mathrm{diag}\left[f_1(r_0), \ldots, f_{N_e}(r_0), F^0_1(X_0), \ldots, F^0_{N_n}(X_0)\right], \quad (42)$$

$$\underline{\mathcal{G}} = \mathrm{diag}\left[g_1(r_0), \ldots, g_{N_e}(r_0), G^0_1(X_0), \ldots, G^0_{N_n}(X_0)\right], \quad (43)$$

the short-range K matrix $\underline{K}$ describing the wave function in both fragmentation regions can be expressed by a familiar transformation,

$$\underline{K} = (\underline{\mathcal{F}} - \underline{\mathcal{F}}'\underline{R})(\underline{\mathcal{G}} - \underline{\mathcal{G}}'\underline{R})^{-1}. \quad (44)$$

Because no asymptotic boundary conditions have been enforced up to this point, the independent solutions in both fragmentation regions,

$$\psi_{i'}(X, r) = \sum_{i_e=1}^{N_e} \phi_{i_e}(X)\left[f_{i_e}(r)\delta_{i_e i'} - g_{i_e}(r) K_{i_e i'}\right] + \sum_{i_n=1}^{N_n} \rho_{i_n}(r)\left[F^0_{i_n}(X)\delta_{i_n i'} - G^0_{i_n}(X) K_{i_n i'}\right], \quad (45)$$

contain exponentially growing components for $r \to \infty$ or $X \to \infty$. Within the MQDT formalism the exponentially growing components of $\psi_{i'}$ are canceled by a proper linear combination of these functions. There are two MQDT techniques available to carry out this elimination of closed channels in the case of one-particle fragmentation. The first technique [8,27,42] works with the short-range K matrix (44) or S matrix expressed in asymptotic channels. This procedure leads to a well-known inversion formula for the physical K or S matrix that are defined in the space of open channels. The second technique [21,42,43] is based on the eigenchannel representation of the wave function in the one-particle asymptotic region and it exploits the fact that the asymptotic phases of the eigenchannel solutions are equal in all the channels. In the present two-particle fragmentation procedure we adopt the latter, the eigenchannel approach.

The eigenchannel solutions,

$$\psi_\gamma(X, r) = \sum_{i_e=1}^{N_e} \phi_{i_e}(X) U_{i_e\gamma}\left[f_{i_e}(r)\cos\pi\tau_\gamma - g_{i_e}(r)\sin\pi\tau_\gamma\right] + \sum_{i_n=1}^{N_n} \rho_{i_n}(r) U_{i_n\gamma}\left[F^0_{i_n}(X)\cos\pi\tau_\gamma - G^0_{i_n}(X)\sin\pi\tau_\gamma\right], \quad (46)$$

have common eigenphase in all the electronic and nuclear fragmentation channels [13]. Here $\tan\pi\tau_\gamma$ and $U_{i\gamma}$ are the eigenvalues and the orthonormal eigenvectors of $\underline{K}$ (44), respectively. Physical boundary conditions at $r \to \infty$ and $X \to \infty$ can be enforced by proper linear combination of the eigensolutions, i.e.,

$$\psi(X, r) = \sum_\gamma \psi_\gamma A_\gamma. \quad (47)$$

The coefficients A_γ must be found such that the wave function $\psi(X, r)$ decays exponentially in each closed channel on the electronic fragmentation surface $\mathcal{S}_e$ ($i_e \in Q_e$) and also in every closed channel on the nuclear fragmentation surface $\mathcal{S}_n$, i.e., for $i_n \in Q_n$. Secondly, the wave function (47) must approach the physical eigenchannel solution which requires a common physical eigenphase shift δ in each of the N_e^o open electronic channels ($i_e \in P_e$) and also in every one of the N_n^o open nuclear channels, i.e., for all $i_n \in P_n$. By combining the Coulomb and free-field procedures described in detail in Refs. [42] and [21] it can be shown that there can be no more than $N_e^o + N_n^o$ such coefficient sets A_γ that lead to the $\psi(X, r)$ satisfying all these conditions. These different coefficient sets will be distinguished by a second index that gives a matrix $A_{\gamma\rho}$. Moreover, the column vectors of $\underline{A}$ are eigenvectors of a singular generalized eigenvalue problem,

$$\underline{\Gamma}\,\underline{A} = \underline{\Lambda}\,\underline{A}\tan\underline{\delta}, \quad (48)$$

with

$$\Gamma_{i\gamma} = \begin{cases} U_{i\gamma}\sin(\beta_i + \pi\tau_\gamma), & i \in Q_e \\ U_{i\gamma}(\kappa_i^{-1}\cos\pi\tau_\gamma + \sin\pi\tau_\gamma), & i \in Q_n \\ U_{i\gamma}\sin\pi\tau_\gamma, & i \in P_e \\ U_{i\gamma}K_i^{1/2}\sin\pi\tau_\gamma, & i \in P_n \end{cases}, \quad (49)$$

and

$$\Lambda_{i\gamma} = \begin{cases} 0, & i \in Q_e \\ 0, & i \in Q_n \\ U_{i\gamma}\cos\pi\tau_\gamma, & i \in P_e \\ U_{i\gamma}K_i^{-1/2}\cos\pi\tau_\gamma, & i \in P_n \end{cases}. \quad (50)$$

The MQDT symbol β_i denotes effective Rydberg quantum numbers with respect to the closed-channel thresholds E_i,

$$\beta_i = \frac{\pi}{\sqrt{2(E_i - E)}}. \tag{51}$$

The $K_i^{1/2}$ terms in Eqs. (49) and (50) allow one to write the open eigenchannel solutions in terms of the energy-normalized asymptotic functions in both fragmentation regions as

$$\psi_\rho(X,r) = \sum_{i\in P_e} \phi_i(X) T_{i\rho}[f_i(r)\cos\pi\delta_\rho - g_i(r)\sin\pi\delta_\rho] + \sum_{i\in P_n} \rho_i(r) T_{i\rho}[F_i(X)\cos\pi\delta_\rho - G_i(X)\sin\pi\delta_\rho], \tag{52}$$

where the energy-normalized nuclear functions are related to the analytic functions (38)–(41) by relations [21] $F_i(X) = K_i^{1/2} F_i^0(X)$ and $G_i(X) = K_i^{-1/2} G_i^0(X)$. The transformation matrix of open eigenchannels,

$$T_{i\rho} = \sum_\gamma A_{\gamma\rho}(\Lambda_{i\gamma}\cos\pi\delta_\rho + \Gamma_{i\gamma}\sin\pi\delta_\rho), \tag{53}$$

is orthogonal and it can be made orthonormal by choosing an appropriate normalization of the eigenvectors $\underline{A}$.

The physical scattering matrix $\underline{S}$ has the dimension of $N_e^o + N_n^o$ and it can be obtained from the open eigenchannels as

$$S_{ij} = \sum_\rho T_{i\rho} e^{2i\delta_\rho} T_{j\rho}, \quad i,j \in P_e \cup P_n, \tag{54}$$

leading to vibrationally inelastic and dissociative recombination integral cross sections,

$$\sigma^{VE}_{i\leftarrow j} = \frac{\pi}{2\epsilon_j}|S_{ij} - \delta_{ij}|^2, \quad i,j \in P_e, \tag{55}$$

$$\sigma^{DR}_{i\leftarrow j} = \frac{\pi}{2\epsilon_j}|S_{ij}|^2, \quad i \in P_n, j \in P_e. \tag{56}$$

III. RESULTS AND DISCUSSION

The exact Hamiltonian (25) together with the BOA Hamiltonians (28) and (29) have been diagonalized in the 2D box confined by $R_0 = 15$ bohr radii and $r_2 = 50$ bohr radii. A large electronic box is chosen to properly represent all the electronic states up to $n = 4$ into which the nuclei dissociate for the examined collision energy 0–2 eV.

The 2D basis was represented as a product of one-dimensional B splines [44]. Electronic functions are fairly smooth over all the examined collision energy range and it was sufficient to involve about 50–60 B splines for the electronic coordinate. Momenta are larger in the nuclear coordinate and therefore we needed about 80 B splines to converge the DR into the $n = 2$ state. However, the nuclei have more than 37 eV of kinetic energy when dissociating into the (unphysical) $n = 1$ state and the convergence for this channel required about 200 of B-spline functions.

All the three exact forms of the 2D R matrix (21), (22), and (26) yielded the same numerical results. However, for the repeated evaluation of the R matrix on a dense energy grid, the Wigner-Eisenbud form (26) is the most convenient one.

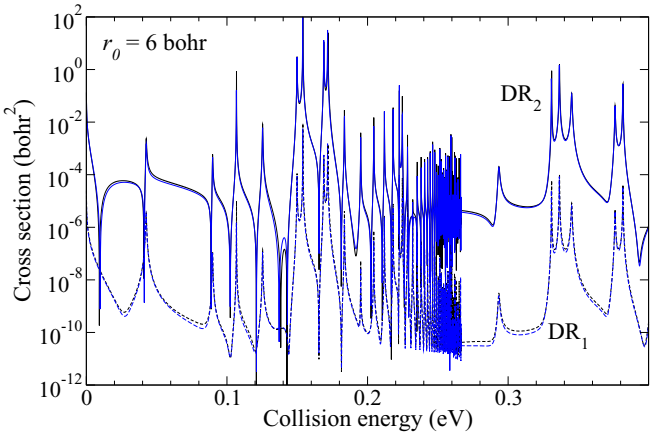

FIG. 2. DR cross sections into final $n = 1$ (broken curves) and $n = 2$ states (full lines). Black lines are exact results, while the blue lines show calculations from the Born-Oppenheimer R matrix and $r_0 = 6$ bohr.

In the second set of calculations the exact R matrix was replaced by its Born-Oppenheimer approximation (35). Since the validity of BOA strongly depends on the electronic box size we need to propagate the R matrix determined at small r_0 to $r_2 = 50$ bohr to satisfy the conditions at which the exact results were obtained. For this we employed the technique devised in the appendix.

In the third set of calculations we attempt to correct the Born-Oppenheimer results by involvement of the first-order nonadiabatic couplings (30) in Eq. (29). Obviously, inclusion of both first-order and second-order (31) couplings reconstructs the exact results accurately.

Comparison between the exact results and the BOA results is shown in Fig. 2. The R-matrix radius $r_0 = 6$ bohr is the lowest possible value that confines the interaction $V(R,r)$ in Eq. (1) and thus it represents the best possible conditions for validity of the BOA. The collision energy range chosen for the demonstration is 0–400 meV. The results were computed and analyzed up to 2 eV and they all follow the conclusions that will be demonstrated on this lower energy window. It is clear that for both DR channels that are open at these energies the BOA R matrix very successfully reconstructs the exact results. For this case we do not show the first-order corrected results because they are practically identical with the exact numbers.

This situation changes already for $r_0 = 12$ bohr. The BOA cross sections displayed in Fig. 3 show visible deviations from the exact results. The dominant $n = 2$ channel cross section is several times lower than the exact results, and the weaker $n = 1$ channel differs by 1–2 orders of magnitude. Once the first-order nonadiabatic coupling terms are included, the results reconstruct the exact numbers accurately. For most of the collision energies shown they are barely distinguishable in Fig. 3.

Validity of the BOA diminishes for $r_0 = 20$ bohr, the $n = 1$ channel is lower by 3–4 orders of magnitude and the $n = 2$ channel starts to miss some of the structures (see Fig. 4). Even

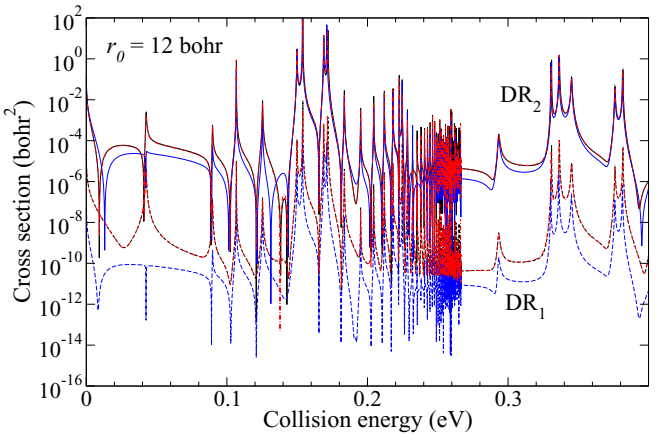

FIG. 3. DR cross sections into final $n = 1$ (broken curves) and $n = 2$ states (full lines). Black lines are exact results, while the blue lines show calculations from the Born-Oppenheimer R matrix and $r_0 = 12$ bohr. Red dot-dashed curves represent results with first-order nonadiabatic couplings included.

inclusion of the first-order couplings starts to show small but visible differences when compared to the exact results.

Deterioration of the BOA results at large electronic distances is a general knowledge in the field of molecular physics that deals with the bound states. In case of continuum states the R-matrix poles become denser for larger electronic box radii r_0 as shown in Fig. 5. On the other, Fig. 6 demonstrates that the first-order nonadiabatic coupling elements $\langle\psi'_k|\psi_{k'}\rangle_r$ of Eq. (30) do not follow this behavior as their magnitude is relatively insensitive to the r_0. Therefore it is clear that for increasing electronic box size r_0, the strength of the coupling terms $V^{(1)}_{kk'}(X)$ on the right-hand side of Eq. (29) will become comparable with the spacing of the adiabatic curves of R-matrix poles $E_k(R)$ in Fig. 5. At this moment the Born-Oppenheimer solutions inside the electronic box confined by the r_0 will cease to be valid. Depending on the desired accuracy, the present model indicates that this may happen already for $r_0 < 12$ bohr.

In order to complete the present analysis we have also carried out a similar study for the second, nonreactive channel

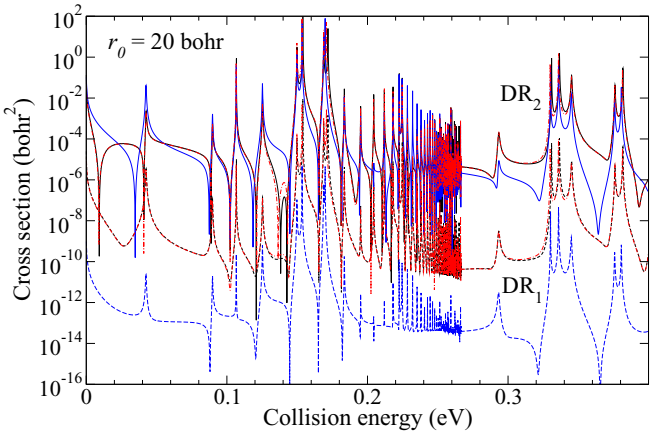

FIG. 4. Same as in Fig. 3 with the radius $r_0 = 20$ bohr.

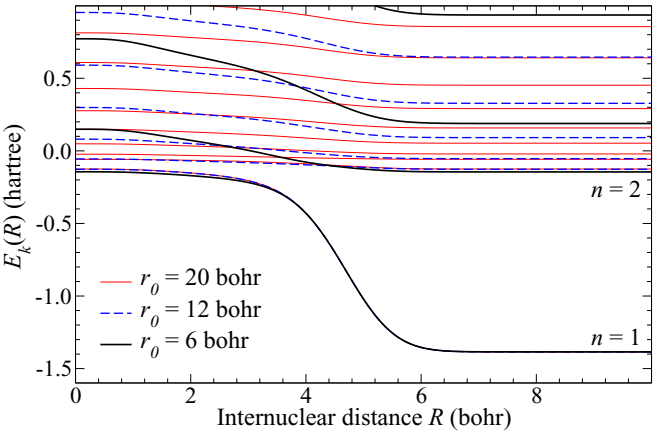

FIG. 5. Fixed-nuclei R-matrix poles $\bar{E}_k(R)$ (28) as a function of the internuclear distance R. Energy curves are shown for three sizes r_0 of the R-matrix box.

that is an inseparable part of the calculations. Figure 7 shows a comparison between the exact electron-impact vibrational excitation cross section and those obtained from the BOA R matrix. The data are displayed for the largest R-matrix radius $r_0 = 20$ bohr. Considering the failure of the Born-Oppenheimer approximation in case of the DR channel displayed in Fig. 4, one observes that the BOA has much weaker impact on the vibrationally inelastic process. Moreover, we do not present the BOA vibrationally inelastic cross sections for smaller R-matrix radii $r_0 = 6$, 12 bohr, because they are practically indistinguishable from the exact results.

IV. CONCLUSIONS

The Born-Oppenheimer approximation is a cornerstone of all the *ab initio* techniques employed in the practical description of elastic and inelastic collisions of electrons with molecules or molecular cations. These techniques involve either the BOA R-matrix method of Schneider *et al.* [28] or various forms of energy-dependent or energy-independent frame transformation methods. It is important to emphasize

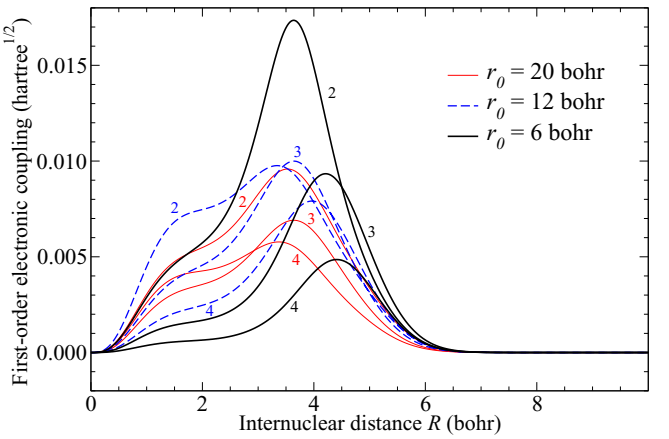

FIG. 6. First-order electronic coupling terms $\langle\psi'_k|\psi_{k'}\rangle_r$ of Eq. (30), where $k' = 1$ and $k = 2,3,4$. Data for three R-matrix box sizes r_0 are displayed.

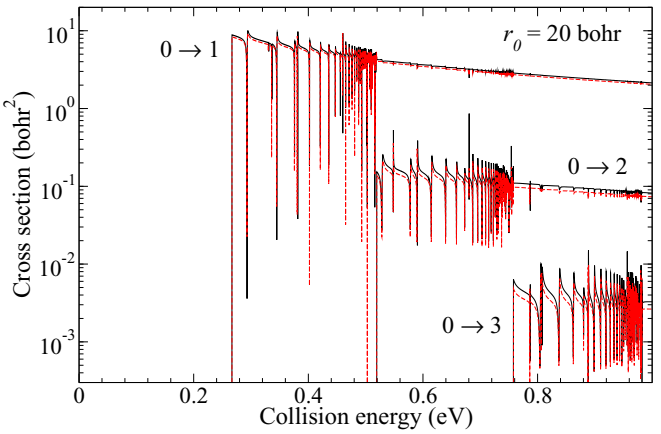

FIG. 7. Vibrationally inelastic cross sections. Full black curves represent the exact results, while the red dashed show calculations from the Born-Oppenheimer R matrix and $r_0 = 20$ bohr.

that in the present study the BOA is considered only at short-range electronic distances $r_0 \leqslant 20$ bohr while the long-range parts of the involved Rydberg states are treated analytically.

In order to assess the validity of the short-range Born-Oppenheimer approximation beyond the experimental accuracy we studied a 2D realistic model describing collisions of electrons with $H_2{}^+$ in the singlet ungerade symmetry. We proposed the 2D R-matrix method to solve this model exactly (within the numerical accuracy) for the dissociative recombination and the vibrational excitation channels. The procedure of the exact solution is separated into two steps.

In the first step all the coupling electron-nuclear interactions are involved in determination of the 2D R matrix on the surface encompassing the region of these interactions. In case this surface is too small to fit the electronic channels in the dissociative process (quite common for the target cations), we also developed a technique to recompute losslessly the R matrix on a surface of a larger 2D box. Since the wave function determined at small distances also contains a contribution from closed channels, these contributions are eliminated simultaneously on the electronic and nuclear surfaces. The elimination of the closed channel represents the full content of the second step.

The exact results then serve as a benchmark for calculations in which the wave functions inside the 2D box are represented by the Born-Oppenheimer products. We demonstrate that for the DR channel the BOA starts to visibly break somewhere between 6 and 12 bohr of the electronic R-matrix radius r_0. Such a narrow validity of the BOA is very impractical because for most of the *ab initio* calculations we expect $r_0 > 15$ bohr for all the internuclear distances R involved. We also show that the first-order nonadiabatic coupling terms correct the inaccuracy of the BOA up to the highest studied $r_0 = 20$ bohr. However, such couplings are very difficult to implement in the present *ab initio* R-matrix codes [45]. The need for the nonadiabatic coupling terms was already recognized by Sarpal *et al.* [4], who used the diabatic representation to numerically estimate the nonadiabatic couplings.

We also demonstrate that the situation is much better in case of the vibrational excitation channels. The discrepancies between the exact and BOA results, found for the largest R-matrix radius $r_0 = 20$ bohr, are less than 10% for the dominant $0 \to 1$ transition.

ACKNOWLEDGMENTS

R.Č. and D.H. conducted this work with support from the Grant Agency of Czech Republic (Grant No. GACR 18-02098S). The contributions of C.H.G. were supported in part by the US Department of Energy, Office of Science, under Grant No. DE-SC0010545.

APPENDIX: R-MATRIX PROPAGATION IN TWO DIMENSIONS

The aim of this appendix is to derive a technique that allows one to recompute an R matrix defined on the surface of Box A (see Fig. 8) to the surface of Box B. As can be seen in Fig. 8, Box A is surrounded by surfaces $\mathcal{S}_1$ and $\mathcal{S}_4$, while the complete set of the orthonormal functions on the surface encompassing Box B is formed from subsets defined on surfaces $\mathcal{S}_2$, $\mathcal{S}_3$, and $\mathcal{S}_4$.

The derivation here is a straightforward generalization of the one-dimensional R-matrix propagator by Baluja *et al.* [41]. A technique similar to the one presented here was also implemented by Scott *et al.* [46] for a two-dimensional R-matrix propagation. Their procedure is tailored for two indistinguishable particles (electrons) while the present model deals with one electronic and one nuclear degree of freedom.

In the first step we diagonalize the symmetrized Hamiltonian in Segment C formed by the difference between Box B and Box A. Before the diagonalization the total Hamiltonian (11) needs to be symmetrized by the Bloch operator,

$$L = \frac{1}{2}\left[\delta(X-X_0)\frac{\partial}{\partial X} + \delta(r-r_2)\frac{\partial}{\partial r} - \delta(r-r_0)\frac{\partial}{\partial r}\right], \quad \text{(A1)}$$

which ensures that $H + L$ is Hermitian on Segment C for functions with arbitrary boundary conditions on surfaces $\mathcal{S}_1$, $\mathcal{S}_2$, and $\mathcal{S}_3$.

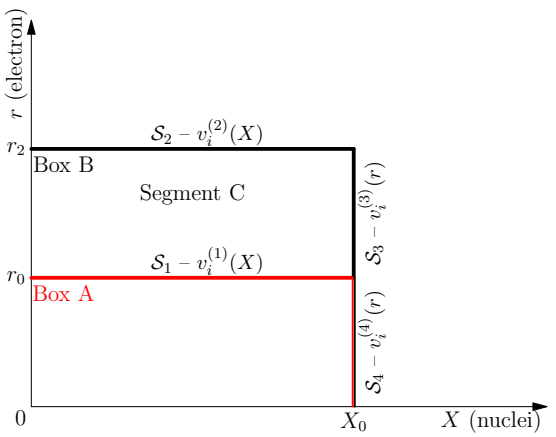

FIG. 8. Propagation of the 2D R matrix from Box A to Box B. The two boxes share the surface $\mathcal{S}_4$. Functions $v^{(\alpha)}$ denote a complete set of orthonormal functions defined on the respective surface $\mathcal{S}_\alpha$.

$\underline{R}_{\mathrm{B}}^{\alpha\beta} =$

α \ β	2	3	4
2	$\underline{\mathcal{R}}^{22} - \underline{\mathcal{R}}^{21}\,\underline{B}\,\underline{\mathcal{R}}^{12}$	$\underline{\mathcal{R}}^{23} - \underline{\mathcal{R}}^{21}\,\underline{B}\,\underline{\mathcal{R}}^{13}$	$\underline{\mathcal{R}}^{21}\,\underline{B}\,\underline{R}_{\mathrm{A}}^{14}$
3		$\underline{\mathcal{R}}^{33} - \underline{\mathcal{R}}^{31}\,\underline{B}\,\underline{\mathcal{R}}^{13}$	$\underline{\mathcal{R}}^{31}\,\underline{B}\,\underline{R}_{\mathrm{A}}^{14}$
4			$\underline{R}_{\mathrm{A}}^{44} - \underline{R}_{\mathrm{A}}^{41}\,\underline{B}\,\underline{R}_{\mathrm{A}}^{14}$

FIG. 9. Matrix elements of the Block B R matrix constructed on surfaces $\mathcal{S}_2$, $\mathcal{S}_3$, and $\mathcal{S}_4$.

After diagonalization of the $H + L$ operator in Segment C,

$$(H + L)|u_p\rangle = E_p|u_p\rangle, \tag{A2}$$

the solution of the Schrödinger equation (7) can be expanded in Segment C as

$$|u\rangle = \sum_p |u_p\rangle \frac{\langle u_p|L|u\rangle}{E_p - E}. \tag{A3}$$

Furthermore, the solution $|u\rangle$ and its surface derivative can be evaluated on the surfaces $\mathcal{S}_1$, $\mathcal{S}_2$, $\mathcal{S}_3$ surrounding Segment C and then projected onto the respective complete set of surface functions $v_i^{(\alpha)}$ ($\alpha = 1, 2, 3$) as

$$u_i^{\alpha} = \left(v_i^{(\alpha)}|u\right), \quad u_i'^{\alpha} = \left(v_i^{(\alpha)}|u'\right), \tag{A4}$$

where u' is a normal derivative on the respective surface and $(.|.)$ denotes the scalar product over the surface coordinate. Surface projections of Eq. (A3) can be now written in the following compact vector equation:

$$u^{\alpha} = -\underline{\mathcal{R}}^{\alpha 1}.u'^{1} + \underline{\mathcal{R}}^{\alpha 2}.u'^{2} + \underline{\mathcal{R}}^{\alpha 3}.u'^{3}, \quad \alpha = 1, 2, 3. \tag{A5}$$

Matrix elements of the six independent matrices $\underline{\mathcal{R}}^{\alpha\beta}$ are

$$\mathcal{R}_{ij}^{\alpha\beta} = \frac{1}{2}\sum_p \frac{\left(v_i^{(\alpha)}|u_p\right)\left(u_p|v_j^{(\beta)}\right)}{E_p - E}, \quad \alpha = 1, 2, 3. \tag{A6}$$

An input for the propagation procedure presented here is the R matrix $\underline{R}_{\mathrm{A}}$ for Box A coupling the values and the normal derivatives on surfaces $\mathcal{S}_1$ and $\mathcal{S}_4$ as

$$u^{\alpha} = \underline{R}_{\mathrm{A}}^{\alpha 1}.u'^{1} + \underline{R}_{\mathrm{A}}^{\alpha 4}.u'^{4}, \quad \alpha = 1, 4. \tag{A7}$$

The R matrix $\underline{R}_{\mathrm{B}}$ for Box B will couple the surfaces $\mathcal{S}_2$, $\mathcal{S}_3$, and $\mathcal{S}_4$ via

$$u^{\alpha} = \underline{R}_{\mathrm{B}}^{\alpha 2}.u'^{2} + \underline{R}_{\mathrm{B}}^{\alpha 3}.u'^{3} + \underline{R}_{\mathrm{B}}^{\alpha 4}.u'^{4}, \quad \alpha = 2, 3, 4. \tag{A8}$$

Combining Eqs. (A5), (A7), and (A8) we arrive at the matrix elements of $\underline{R}_{\mathrm{B}}^{\alpha\beta}$ shown in Fig. 9, with the matrix $\underline{B}$ defined on the surface $\mathcal{S}_1$ as

$$\underline{B} = \left(\underline{\mathcal{R}}^{11} + \underline{R}_{\mathrm{A}}^{11}\right)^{-1}. \tag{A9}$$

From the definition of matrices $\mathcal{R}_{ij}^{\alpha\beta}$ (A6) it is clear that the result of the 2D propagation, the matrix $\underline{R}_{\mathrm{B}}$ is Hermitian on the surface surrounding Box B, provided the matrix $\underline{R}_{\mathrm{A}}$ was Hermitian in the first place.

We conclude this section with two remarks of a technical nature.

(1) While we have not assumed any particular form of the Hamiltonian (A2) diagonalized in Segment C, in most of the practical applications as in the present study, the Hamiltonian H becomes separable in the nuclear and electronic coordinates. This trivializes the formal 2D diagonalization in (A2) to two one-dimensional diagonalizations. In such a case the cost of all the operations needed to recompute the 2D R matrix from Box A to Box B is $\sim N^3$, where N is the size of the one-dimensional basis. It can be compared to the cost $\sim N^6$ of the 2D diagonalization inside Box A.

(2) The final form of the $\underline{R}_{\mathrm{B}}$ matrix displayed in Fig. 9 is expressed in a complete set of orthonormal channels on the surface of Box B. However, these channels do not represent the physical channels into which the nuclei dissociate. The matrix $\underline{R}_{\mathrm{B}}$ needs to be transformed into the proper physical channels (19) and (20) defined on the surface surrounding Box B as

$$(R_{\mathrm{B}})_{ij} = \sum_{\alpha,\beta=2}^{4} (i|v^{(\alpha)}).\underline{R}_{\mathrm{B}}^{\alpha\beta}.(v^{(\beta)}|j). \tag{A10}$$

[1] D. R. Bates, Phys. Rep. **78**, 492 (1950).
[2] P. C. Stancil, S. Lepp, and A. Dalgarno, Astrophys. J. **458**, 401 (1996).
[3] S. L. Guberman, Phys. Rev. A **49**, R4277 (1994).
[4] B. K. Sarpal, J. Tennyson, and L. A. Morgan, J. Phys. B: At. Mol. Opt. Phys. **27**, 5943 (1994).
[5] I. F. Schneider, A. E. Orel, and A. Suzor-Weiner, Phys. Rev. Lett. **85**, 3785 (2000).
[6] V. Kokoouline and C. H. Greene, Phys. Rev. A **68**, 012703 (2003).
[7] A. Giusti-Suzor, J. N. Bardsley, and C. Derkits, Phys. Rev. A **28**, 682 (1983).
[8] K. Nakashima, H. Takagi, and H. Nakamura, J. Chem. Phys. **86**, 726 (1987).
[9] I. F. Schneider, O. Dulieu, and A. Giusti-Suzor, J. Phys. B: At. Mol. Opt. Phys. **24**, L289 (1991).
[10] R. Čurík and F. A. Gianturco, Phys. Rev. A **87**, 012705 (2013).
[11] V. Kokoouline and C. H. Greene, Phys. Rev. A **72**, 022712 (2005).
[12] T. Tanabe, I. Katayama, S. Ono, K. Chida, T. Watanabe, Y. Arakaki, Y. Haruyama, M. Saito, T. Odagiri, K. Hosono *et al.*, J. Phys. B: At. Mol. Opt. Phys. **31**, L297 (1998).
[13] C. Jungen and S. C. Ross, Phys. Rev. A **55**, R2503(R) (1997).

[14] J. Z. Mezei, F. Colboc, N. Pop, S. Ilie, K. Chakrabarti, S. Niyonzima, M. Lepers, A. Bultel, O. Dulieu, O. Motapon *et al.*, Plasma Sources Sci. Technol. **25**, 055022 (2016).
[15] E. S. Chang and U. Fano, Phys. Rev. A **6**, 173 (1972).
[16] J. Semaniak, S. Rosen, G. Sundstrom, C. Stromholm, S. Datz, H. Danared, M. af Ugglas, M. Larsson, W. J. van der Zande, Z. Amitay *et al.*, Phys. Rev. A **54**, R4617 (1996).
[17] K. Chakrabarti, J. Z. Mezei, O. Motapon, A. Faure, O. Dulieu, K. Hassouni, and I. F. Schneider, J. Phys. B: At. Mol. Opt. Phys. **51**, 104002 (2018).
[18] R. Čurík and C. H. Greene, J. Chem. Phys. **147**, 054307 (2017).
[19] R. von Hahn, A. Becker, F. Berg, K. Blaum, C. Breitenfeldt, H. Fadil, F. Fellenberger, M. Froese, S. George, J. Goeck *et al.*, Rev. Sci. Instrum. **87**, 063115 (2016).
[20] H. Gao and C. H. Greene, Phys. Rev. A **42**, 6946 (1990).
[21] H. Gao and C. Greene, J. Chem. Phys. **91**, 3988 (1989).
[22] C. H. Greene and C. Jungen, Phys. Rev. Lett. **55**, 1066 (1985).
[23] D. Hvizdoš, M. Váňa, K. Houfek, C. H. Greene, T. N. Rescigno, C. W. McCurdy, and R. Čurík, Phys. Rev. A **97**, 022704 (2018).
[24] K. Houfek, T. N. Rescigno, and C. W. McCurdy, Phys. Rev. A **73**, 032721 (2006).
[25] K. Houfek, T. N. Rescigno, and C. W. McCurdy, Phys. Rev. A **77**, 012710 (2008).
[26] M. J. Seaton, Rep. Prog. Phys. **46**, 167 (1983).
[27] M. Aymar, C. H. Greene, and E. Luc-Koenig, Rev. Mod. Phys. **68**, 1015 (1996).
[28] B. I. Schneider, M. LeDourneuf, and P. G. Burke, J. Phys. B: At. Mol. Phys. **12**, L365 (1979).
[29] B. I. Schneider, M. LeDourneuf, and V. K. Lan, Phys. Rev. Lett. **43**, 1926 (1979).
[30] L. A. Morgan, J. Phys. B: At. Mol. Phys. **19**, L439 (1986).
[31] L. A. Morgan, J. Phys. B: At. Mol. Opt. Phys. **24**, 4649 (1991).
[32] B. K. Sarpal, J. Tennyson, and L. A. Morgan, J. Phys. B: At. Mol. Opt. Phys. **24**, 1851 (1991).
[33] I. Rabadán and J. Tennyson, J. Phys. B: At. Mol. Opt. Phys. **32**, 4753 (1999).
[34] C. Jungen and O. Atabek, J. Chem. Phys. **66**, 5584 (1977).
[35] E. L. Hamilton, Ph.D thesis, University of Colorado, 2003.
[36] R. Szmytkowski, Phys. Rev. A **66**, 029901(E) (2002).
[37] R. Nesbet, *Variational Methods in Electron-Atom Scattering Theory*, Physics of Atoms and Molecules (Plenum Press, New York, 1980).
[38] F. Robicheaux, Phys. Rev. A **43**, 5946 (1991).
[39] E. P. Wigner and L. Eisenbud, Phys. Rep. **72**, 29 (1947).
[40] C. Jungen, Phys. Rev. Lett. **53**, 2394 (1984).
[41] K. L. Baluja, P. G. Burke, and L. A. Morgan, Comput. Phys. Commun. **27**, 299 (1982).
[42] C. H. Greene and C. Jungen, in *Advances in Atomic and Molecular Physics*, Vol. 21 (Academic Press, Cambridge, 1985), pp. 51–121.
[43] K. T. Lu, Phys. Rev. A **4**, 579 (1971).
[44] H. Bachau, E. Cormier, P. Decleva, J. E. Hansen, and F. Martín, Rep. Prog. Phys. **64**, 1815 (2001).
[45] L. A. Morgan, C. J. Gillan, J. Tennyson, and X. S. Chen, J. Phys. B: At. Mol. Opt. Phys. **30**, 4087 (1997).
[46] N. Scott, M. Scott, P. Burke, T. Stitt, V. Faro-Maza, C. Denis, and A. Maniopoulou, Comput. Phys. Commun. **180**, 2424 (2009).